Acta Crystallographica Section B
Structural Science
ISSN 0108-7681

A structural study of new potent and selective antagonists to the A_{2B} adenosine receptor

Valeria Ferretti,[a]* Loretta Pretto,[a] Mojgan Aghazadeh Tabrizi[b] and Valerio Bertolasi[a]

[a]Dipartimento di Chimica and Centro di Strutturistica Diffrattometrica, University of Ferrara, via L. Borsari 46, I-44100 Ferrara, Italy, and [b]Dipartimento di Scienze Farmaceutiche, University of Ferrara, via Fossato di Mortara 17-19, I-44100 Ferrara, Italy

Correspondence e-mail: frt@unife.it

Received 4 April 2005
Accepted 4 July 2005

Xanthines, including the natural derivatives theophylline and caffeine, are non-selective antagonists of adenosine. They are able to bind with good affinity to all four adenosine-receptor subtypes A_1, A_{2A}, A_{2B} and A_3. In order to develop new drugs with few side effects, over the last few years many efforts have been devoted to the discovery of new adenosine antagonists with enhanced selectivity properties. The present paper reports the crystal structures of five new xanthinic derivatives, which display different affinities and selectivity properties towards the A_{2B} receptor. Besides the crystallographic study, a structural comparison has been made with the calculated geometry of other xanthinic derivatives which are reported to have similar biological characteristics to understand the structural features controlling their affinity capabilities and selectivity. This structural comparison has been interpreted in the light of a recently published study on the binding of *N*-benzo[1,3]-dioxol-5-yl-2-[5-(2,6-dioxo-1,3-dipropyl-2,3,6,9-tetrahydro-1*H*-purin-8-yl)-1-methyl-1-*H*-pyrazol-3-iloxy]-acetamide to a model of the A_{2B} receptor, which shows the most interesting affinity and selectivity properties.

1. Introduction

The rhodopsin-like adenosine receptors belong to the superfamily of G-protein-coupled receptors (Beck-Sickinger, 1996). On the basis of their distinct molecular structures they are further divided into four subtypes, A_1, $A_{2A,}$ A_{2B} and A_3, which show different tissue distributions and pharmacological profiles. The proposed membrane structure is characterized by seven *trans*-membrane domains (7TM) with an α-helix structure, connected by three extracellular and three intracellular loops. The extracellular *N*-terminal segment of these proteins is highly glycosylated and a number of polar residues within the transmembrane segments, probably involved in a hydrogen-bond network, are conserved. The second intracellular loop and parts of the third intracellular loop of the *C*-terminal segment are involved in G-protein interactions and therefore in signal transduction. The endogenous agonist adenosine is believed to bind within the upper part of the pocket formed by the three-dimensional arrangement of the transmembrane α-helices (Ralevic & Burnstock, 1998). There is evidence that residues in the extracellular loops could also be involved in the early stages of ligand recognition (Kim *et al.*, 1996). Of the 7TM superfamily receptors, only bovine rhodopsin has been structurally characterized (Palczewski *et al.*, 2000), confirming the presence of a highly organized heptahelical transmembrane bundle where the retinal molecule is bound.

Table 1
Experimental details.

	(1)	(2)	(3)	(4)	(5)
Crystal data					
Chemical formula	$C_{24}H_{27}N_7O_6\cdot CH_4N_2O\cdot H_2O$	$C_{27}H_{30}N_8O_4$	$C_{23}H_{27}N_7O_3$	$C_{22}H_{25}ClN_8O_3\cdot H_2O\cdot\cdot C_3H_7NO$	$C_{24}H_{29}N_7O_3\cdot 2H_2O$
M_r	587.60	530.59	449.52	594.08	499.57
Cell setting, space group	Triclinic, $P\overline{1}$	Triclinic, $P\overline{1}$	Monoclinic, $C2/c$	Triclinic, $P\overline{1}$	Monoclinic, $P2_1/a$
a, b, c (Å)	7.6900 (2), 9.6995 (2), 20.1404 (5)	8.7035 (2), 12.4960 (3), 13.7034 (3)	33.9318 (5), 5.0250 (1), 30.4072 (6)	10.5330 (2), 11.1912 (2), 14.2829 (4)	10.4021 (3), 15.3698 (6), 16.6432 (7)
α, β, γ (°)	80.5220 (10), 86.7920 (10), 72.3300 (16)	63.4160 (10), 89.9970 (10), 78.2200 (9)	90.00, 122.6890 (8), 90.00	85.5320 (10), 81.8420 (11), 63.0190 (13)	90.00, 99.0850 (16), 90.00
V (Å^3)	1411.81 (6)	1297.62 (5)	4363.47 (14)	1485.02 (6)	2627.50 (17)
Z	2	2	8	2	4
D_x (Mg m^{-3})	1.382	1.358	1.369	1.329	1.263
Radiation type	Mo $K\alpha$	Mo $K\alpha$	Mo $K\alpha$	Mo $K\alpha$	Mo $K\alpha$
No. of reflections for cell parameters	10 620	7632	8460	11 842	10 036
θ range (°)	3.0–28.0	3.8–28	4.0–28.0	3.4–28.0	3.0–27.0
μ (mm^{-1})	0.11	0.10	0.10	0.18	0.09
Temperature (K)	295	295	150	295	295
Crystal form, colour	Plate, colourless	Plate, colourless	Plate, colourless	Plate, colourless	Plate, colourless
Crystal size (mm)	0.49 × 0.25 × 0.10	0.44 × 0.15 × 0.09	0.32 × 0.25 × 0.07	0.38 × 0.20 × 0.12	0.41 × 0.17 × 0.06
Data collection					
Diffractometer	Nonius Kappa CCD	Nonius Kappa CCD	Nonius Kappa CCD	Nonius Kappa CCD	Nonius Kappa CCD
Data collection method	φ scans and ω scans	φ scans and ω scans	φ scans and ω scans	φ scans and ω scans	φ scans and ω scans
Absorption correction	None	None	None	None	None
No. of measured, independent and observed reflections	10 620, 6675, 4559	7632, 6218, 4642	8460, 4960, 3001	11 842, 6870, 4703	9233, 5660, 3630
Criterion for observed reflections	$I > 2\sigma(I)$	$I > 2\sigma(I)$	$I > 2\sigma(I)$	$I > 2\sigma(I)$	$I > 2\sigma(I)$
R_{int}	0.034	0.025	0.043	0.034	0.038
θ_{max} (°)	28.0	28.0	27.5	28.0	27.0
Range of h, k, l	$0 \Rightarrow h \Rightarrow 10$ $-11 \Rightarrow k \Rightarrow 12$ $-26 \Rightarrow l \Rightarrow 26$	$-11 \Rightarrow h \Rightarrow 11$ $-16 \Rightarrow k \Rightarrow 16$ $-18 \Rightarrow l \Rightarrow 18$	$-43 \Rightarrow h \Rightarrow 44$ $-5 \Rightarrow k \Rightarrow 6$ $-38 \Rightarrow l \Rightarrow 38$	$0 \Rightarrow h \Rightarrow 13$ $-12 \Rightarrow k \Rightarrow 14$ $-18 \Rightarrow l \Rightarrow 18$	$0 \Rightarrow h \Rightarrow 13$ $-17 \Rightarrow k \Rightarrow 19$ $-21 \Rightarrow l \Rightarrow 20$
Refinement					
Refinement on	F^2	F^2	F^2	F^2	F^2
$R[F^2 > 2\sigma(F^2)]$, $wR(F^2)$, S	0.052, 0.151, 1.04	0.048, 0.139, 1.07	0.050, 0.131, 1.01	0.055, 0.169, 1.03	0.065, 0.213, 1.02
No. of reflections	6675	6218	4960	6870	5660
No. of parameters	477	461	402	459	374
H-atom treatment	Mixture of independent and constrained refinement	Mixture of independent and constrained refinement	Mixture of independent and constrained refinement	Mixture of independent and constrained refinement	Mixture of independent and constrained refinement
Weighting scheme	$w = 1/[\sigma^2(F_o^2) + (0.0591P)^2 + 0.2999P]$, where $P = (F_o^2 + 2F_c^2)/3$	$w = 1/[\sigma^2(F_o^2) + (0.056P)^2 + 0.4213P]$, where $P = (F_o^2 + 2F_c^2)/3$	$w = 1/[\sigma^2(F_o^2) + (0.0589P)^2 + 2.0736P]$, where $P = (F_o^2 + 2F_c^2)/3$	$w = 1/[\sigma^2(F_o^2) + (0.0733P)^2 + 0.4729P]$, where $P = (F_o^2 + 2F_c^2)/3$	$w = 1/[\sigma^2(F_o^2) + (0.1063P)^2 + 0.5378P]$, where $P = (F_o^2 + 2F_c^2)/3$
$(\Delta/\sigma)_{max}$	0.001	0.004	0.006	0.001	0.001
$\Delta\rho_{max}$, $\Delta\rho_{min}$ (e Å^{-3})	0.19, −0.17	0.32, −0.26	0.33, −0.29	0.25, −0.43	0.39, −0.20

Computer programs used: *Kappa CCD server software* (Nonius, 1997), *DENZO-SMN* (Otwinowski & Minor, 1997), *SIR*97 (Altomare *et al.*, 1999), *SHELXL*97 (Sheldrick, 1997), *ORTEP*III (Burnett & Johnson, 1996), *PARST* (Nardelli, 1995), *WINGX* (Farrugia, 1999).

Adenosine A_{2B} receptors are implicated in mast-cell activation and asthma, vasodilatation, regulation of cell growth, intestinal function, and modulation of neurosecretion, and have been classified as 'low-affinity' receptors because of the high adenosine concentrations required for their activation (Bruns *et al.*, 1986). The receptors were cloned in the 1990s from rat hypothalamus (Rivkees & Reppert, 1992), human hippocampus (Pierce *et al.*, 1992) and mouse mast cells

Table 2
Selected bond distances (Å) and angles (°) for (1)–(5).

	(1)	(2)	(3)	(4)	(5)
O1—C2	1.215 (2)	1.217 (2)	1.220 (2)	1.220 (3)	1.221 (3)
O2—C6	1.231 (2)	1.234 (2)	1.234 (3)	1.236 (3)	1.226 (3)
N1—C2	1.410 (2)	1.406 (2)	1.402 (3)	1.404 (3)	1.395 (3)
N1—C6	1.394 (2)	1.396 (2)	1.404 (2)	1.398 (3)	1.403 (3)
N1—C10	1.475 (2)	1.469 (2)	1.477 (3)	1.479 (4)	1.476 (4)
N3—C2	1.378 (2)	1.379 (2)	1.382 (3)	1.375 (4)	1.386 (3)
N3—C4	1.375 (2)	1.371 (2)	1.372 (2)	1.374 (3)	1.379 (3)
N3—C13	1.476 (2)	1.469 (2)	1.467 (4)	1.471 (3)	1.468 (4)
N7—C5	1.378 (2)	1.379 (2)	1.383 (2)	1.381 (3)	1.381 (3)
N7—C9	1.352 (2)	1.355 (2)	1.360 (3)	1.351 (3)	1.350 (3)
N8—C4	1.354 (2)	1.357 (2)	1.356 (3)	1.356 (3)	1.355 (3)
N8—C9	1.339 (2)	1.342 (2)	1.344 (2)	1.342 (2)	1.340 (3)
N9—N10	1.361 (2)	1.368 (2)	1.365 (2)	1.362 (3)	1.360 (2)
N9—C16	1.346 (2)	1.354 (2)	1.359 (3)	1.355 (3)	1.354 (3)
N9—C19	1.462 (3)	1.453 (2)	1.460 (3)	1.454 (3)	1.452 (3)
N10—C18	1.322 (2)	1.325 (2)	1.338 (3)	1.336 (2)	1.325 (3)
C4—C5	1.362 (2)	1.367 (2)	1.366 (3)	1.365 (3)	1.365 (3)
C5—C6	1.415 (2)	1.409 (2)	1.424 (3)	1.413 (4)	1.408 (3)
C9—C16	1.452 (2)	1.450 (2)	1.450 (3)	1.453 (4)	1.453 (3)
C16—C17	1.384 (2)	1.376 (2)	1.382 (3)	1.383 (3)	1.386 (3)
C17—C18	1.386 (2)	1.394 (2)	1.394 (3)	1.390 (4)	1.393 (3)
C2—N1—C6	126.6 (1)	126.1 (1)	126.7 (2)	125.9 (2)	126.5 (2)
C2—N1—C10	116.7 (1)	115.8 (1)	117.0 (2)	115.9 (2)	115.8 (2)
C6—N1—C10	116.7 (1)	118.1 (1)	116.3 (2)	118.2 (2)	117.7 (2)
C2—N3—C4	119.8 (1)	119.7 (1)	119.4 (2)	119.2 (2)	119.0 (2)
C2—N3—C13	120.0 (2)	118.7 (1)	118.8 (2)	118.6 (2)	120.3 (2)
C4—N3—C13	120.1 (1)	121.6 (1)	121.7 (2)	122.2 (2)	120.6 (2)
C5—N7—C9	106.0 (1)	106.2 (1)	106.2 (2)	106.5 (2)	106.2 (2)
C4—N8—C9	103.1 (1)	103.6 (1)	103.6 (2)	103.4 (2)	103.6 (2)
O1—C2—N1	121.2 (1)	121.0 (1)	122.0 (2)	120.7 (2)	121.4 (2)
O1—C2—N3	122.3 (2)	122.0 (1)	121.1 (2)	121.7 (2)	121.4 (2)
N1—C2—N3	116.5 (2)	117.0 (1)	116.8 (2)	117.6 (2)	117.2 (2)
N3—C4—N8	126.0 (2)	126.5 (1)	125.2 (2)	125.9 (2)	126.2 (2)
N3—C4—C5	121.4 (2)	121.4 (1)	122.4 (2)	121.7 (2)	121.7 (2)
N8—C4—C5	112.6 (2)	112.1 (1)	112.4 (2)	112.4 (2)	112.1 (2)
N7—C5—C4	105.2 (1)	105.4 (1)	105.3 (2)	105.0 (2)	105.3 (2)
N7—C5—C6	131.4 (2)	131.2 (1)	132.1 (2)	131.6 (2)	131.2 (2)
C4—C5—C6	123.4 (2)	123.3 (1)	122.5 (2)	123.3 (2)	123.3 (2)
O2—C6—N1	121.6 (2)	121.3 (1)	120.6 (2)	120.7 (2)	120.9 (2)
O2—C6—C5	126.3 (2)	126.2 (1)	127.3 (2)	127.0 (2)	126.9 (2)
N1—C6—C5	112.0 (1)	112.4 (1)	112.0 (2)	112.3 (2)	112.2 (2)
N7—C9—N8	113.1 (1)	112.7 (1)	112.5 (2)	112.7 (2)	112.8 (2)
N7—C9—C16	120.6 (2)	120.1 (1)	123.3 (2)	120.6 (2)	120.8 (2)
N8—C9—C16	126.3 (2)	127.1 (1)	124.2 (2)	126.7 (2)	126.3 (2)

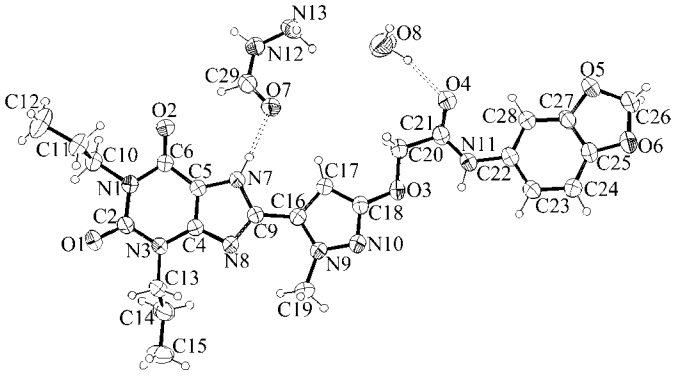

Figure 1
*ORTEP*III (Burnett & Johnson, 1996) view and atom numbering for (1). The displacement ellipsoids are drawn at 40% probability.

(Marquardt *et al.*, 1994). The highest degree of identity in amino-acid sequences among A_{2B} receptors of different species was found in the transmembrane domain, where the binding pocket is presumably located. Some indications about the nature of the residues that are presumably involved in ligand binding can be found from the very few site-mutagenesis studies presently available (for a review on site-mutagenesis studies, see Fredholm *et al.*, 2001), but the ligand–receptor binding modalities are still almost unknown.

Although highly selective and potent agonists have been designed for A_1, A_{2A} and A_3, no selective agonist for the A_{2B} receptor has been found so far. As for the antagonists, the therapeutic use of simple xanthines such as theophilline in the treatment of asthma has been found to produce strong side effects. For these reasons many efforts have been devoted in the last few years to developing new antagonists with good affinity for the A_{2B} receptor, mostly belonging to the chemical classes of xanthinic (Kim *et al.*, 2000, 2002; Hayallah *et al.*, 2002; Baraldi *et al.*, 2004) and pyrazolo derivatives (Kim *et al.*, 1998; Baraldi *et al.*, 2002), in an attempt to enhance their selectivity in addition to affinity. We present here the crystal structures of five new xanthinic derivatives: *N*-benzo[1,3]-dioxol-5-yl-2-[5-(2,6-dioxo-1,3-dipropyl-2,3,6,9-tetrahydro-1*H*-purin-8-yl)-1-methyl-1-*H*-pyrazol-3-iloxy]-acetamide (1); 1,3-diallyl-8-{2-methyl-5-[2-oxo-2-(4-phenylpyperazin-1-yl)-ethoxyl]2*H*-pyrazol-3-yl}-3,9-dihydro-purin-2,6-dione (2); *N*-[5-(2,6-dioxo-1,3-dipropyl-2,3,6,9-tetrahydro-1*H*-purin-8-yl)-1-methyl-1-*H*-pyrazol-3yl]2-phenyl acetamide (3); 1-(3-chloro-phenyl)-3-[5-(2,6-dioxo-1,3-dipropyl-2,3,6,9-tetrahydro-1*H*-purin-8-yl)-1-methyl-1*H*-pyrazol-3-yl]urea (4) and *N*-[5-(2,6-dioxo-1,3-dipropyl-2,3,6,9-tetrahydro-1*H*-purin-8-yl)-1-methyl-1*H*-pyrazol-3-yl]2-phenyl propionamide (5). These five compounds exhibit very different affinity and selectivity properties towards the A_{2B} receptor subtype. We also present a structural comparison with some molecules belonging to the same chemical class to understand the structural features controlling their affinity capabilities and selectivity. The results of this structural comparison have been interpreted in light of our recent study in which (1) has been docked to a model of the A_{2B} receptor transmembrane domains (Ferretti & Bertoni, 2004).

2. Experimental and computational methods

The syntheses and biological data of the five molecules have been reported elsewhere (Baraldi *et al.*, 2004). Suitable crystals were obtained by slow evaporation at room temperature from a mixture of dimethylformamide (DMF), formylhydrazine and 2-propanol (1), DMF and dicholoroethane (2), DMF and isoamylic alcohol (3), DMF and ethanol (4), and DMF and petroleum ether (5). Crystal data, data collection and refinement parameters are summarized in Table 1[1] and a selection of bond lengths and angles is reported in Table 2. For

[1] Supplementary data for this paper are available from the IUCr electronic archives (Reference: BK5016). Services for accessing these data are described at the back of the journal.

Table 3
Hydrogen-bonding parameters (Å, °).

	D—H	*D*···*A*	H···*A*	*D*—H···*A*
(1)				
O8—H1···O4	0.89 (5)	2.904 (3)	2.04 (4)	164 (4)
N7—H···O7	0.88 (2)	2.770 (2)	1.89 (2)	176 (2)
C17—H···O7	0.92 (2)	3.313 (2)	2.49 (2)	150 (2)
C29—H···O2	0.99 (3)	3.243 (3)	2.41 (3)	141 (2)
N12—H1···N10^{i}	0.92 (2)	2.993 (2)	2.08 (2)	170 (2)
O8—H2···O2^{ii}	1.01 (5)	2.950 (3)	1.95 (6)	168 (4)
N13—H···O7^{ii}	0.92 (4)	3.191 (3)	2.30 (4)	163 (3)
C23—H···...N13^{iii}	0.95 (2)	3.565 (3)	2.64 (2)	164 (2)
(2)				
N7—H···O2^{iv}	0.95 (2)	2.825 (2)	1.88 (2)	174 (2)
C17—H···O2^{iv}	0.95 (2)	3.165 (2)	2.27 (2)	156 (2)
C25—H1···O1^{v}	1.00 (2)	3.56 (2)	2.62 (2)	157 (2)
C19—H1···N12^{vi}	0.96 (3)	3.56 (2)	2.63 (3)	165 (3)
C15—H1···O4^{vii}	0.98 (3)	3.500 (3)	2.53 (3)	169 (2)
(3)				
N7—H···O2^{viii}	0.99 (3)	2.779 (3)	1.80 (3)	169 (3)
N11—H···N10^{ix}	0.92 (3)	3.151 (3)	2.25 (3)	170 (3)
C21—H1···N10^{ix}	0.97 (3)	3.542 (4)	2.67 (3)	150 (2)
C19—H1···N10^{x}	0.96	3.632 (3)	2.70	162
C25—H···O1^{xi}	0.96	3.44 (2)	2.52	169
C15*A*—H1···O1^{xii}	0.96	3.60 (1)	2.65	172
(4)				
O6—H1···O5	0.95 (6)	2.831 (4)	1.90 (6)	166 (5)
N7—H···O6	0.84 (2)	2.787 (3)	1.95 (2)	172 (2)
N11—H···O4	0.87 (3)	2.870 (4)	2.05 (3)	155 (2)
N12—H···O4	0.92 (3)	2.834 (3)	1.97 (3)	157 (2)
C17—H···O6	0.88 (3)	3.390 (3)	2.62 (3)	147 (2)
O5—H1···N10^{xiii}	0.94 (5)	2.917 (3)	1.98 (5)	175 (4)
O5—H2···O2^{xiv}	0.89 (3)	2.777 (3)	1.90 (3)	171 (4)
O6—H2···O5^{xiv}	0.85 (5)	2.872 (4)	2.03 (4)	172 (4)
C13—H1···O3^{xv}	0.98 (3)	3.448 (3)	2.56 (3)	150 (3)
C23—H···O1^{xvi}	0.96 (4)	3.165 (3)	2.47 (3)	130 (3)
(5)				
O4—H1···O5	1.00 (6)	2.839 (3)	1.92 (6)	150 (5)
O5—H1···O3	0.98 (4)	2.751 (3)	1.78 (4)	172 (4)
N7—H···O4	1.00 (3)	2.798 (3)	1.80 (3)	172 (3)
C17—H···O5	0.93 (4)	3.381 (4)	2.58 (4)	144 (3)
N11—H···O5^{xvii}	0.86 (3)	2.852 (3)	2.01 (3)	165 (3)
O5—H2···O2^{xiii}	0.94 (4)	2.717 (3)	1.83 (4)	158 (4)
O4—H2···N10^{xviii}	0.88 (4)	3.002 (3)	2.18 (4)	156 (3)
C19—H1···O2^{xix}	0.93 (4)	3.421 (5)	2.60 (4)	147 (4)

Symmetry codes: (i) $x-1, y+1, z$; (ii) $2-x, 1-y, 1-z$; (iii) $x+1, y-1, z$; (iv) $1-x, -y, -z$; (v) $-x, -y, -z$; (vi) $-x-1, 1-y, -z-1$; (vii) $x, y, 1+z$; (viii) $\frac{1}{2}-x, \frac{3}{2}-y, 1-z$; (ix) $\frac{1}{2}-x, \frac{1}{2}+y, \frac{3}{2}-z$; (x) $x, y-1, z$; (xi) $\frac{1}{2}+x, \frac{3}{2}-y, z+\frac{1}{2}$; (xii) $x, y+1, z$; (xiii) $1-x, -y, 1-z$; (xiv) $1-x, 1-y, 1-z$; (xv) $2-x, -y, 1-z$; (xvi) $x-1, y, z-1$; (xvii) $x, \frac{1}{2}-y, \frac{1}{2}+z$; (xviii) $1-x, y-\frac{1}{2}, \frac{3}{2}-z$; (xix) $x-\frac{1}{2}, \frac{1}{2}-y, z$.

all compounds, the non-H atoms were refined anisotropically and H atoms isotropically, with the exception of the H atoms belonging to the methyl groups or the disordered parts, which were included on calculated positions, riding on their attached atoms. *ORTEP*III (Burnett & Johnson, 1996) views of (1)–(5) are shown in Figs. 1–5. Hydrogen-bonding parameters for the five structures are reported in Table 3. Biological data for (1)–(5) are reported in Table 4. The superposition of the five crystal structures is shown in Fig. 6.

MOPAC-PM3 semiempirical calculations (Stewart, 1989) implemented in the *MOE* (Chemical Computing Group Inc., 2003) system of programs were performed for the geometry optimization of nine molecules (retrieved from the literature), showing affinity and selectivity properties comparable to those of (1). Their formulae and biological data are reported in Table 5. All the molecules have been superimposed on (1) using the *MOE* Flex Align procedure (Wildman & Crippen, 1999; Miller *et al.*, 1999) with the MMFF94 molecular mechanics forcefield (Halgren, 1996; Halgren & Nachbar,

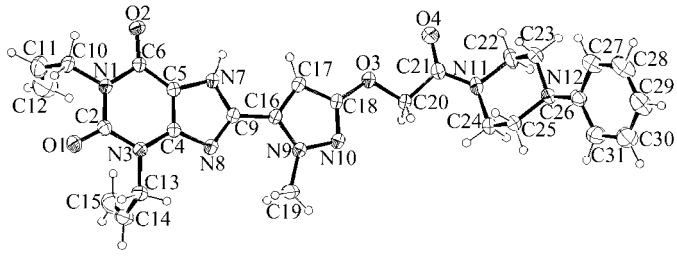

Figure 2
*ORTEP*III view and atom numbering for (2). The displacement ellipsoids are drawn at 40% probability.

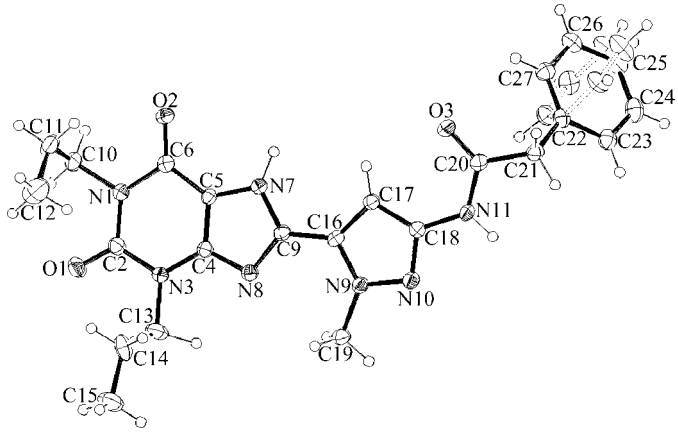

Figure 3
*ORTEP*III view and atom numbering for (3). The displacement ellipsoids are drawn at 40% probability. For the sake of clarity, only one component of the disordered C13—C14—C15 group is shown.

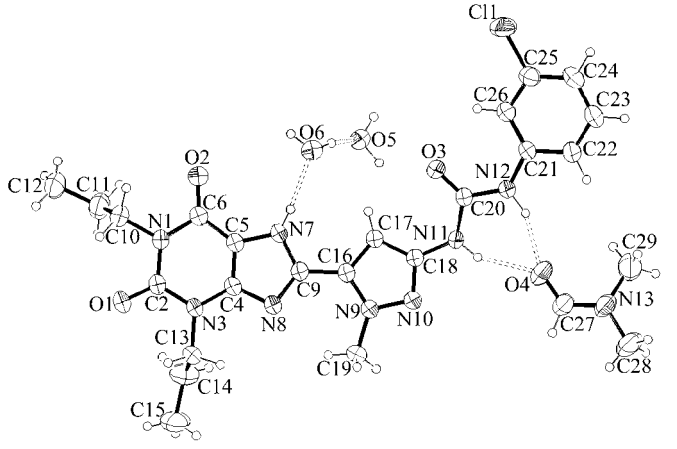

Figure 4
*ORTEP*III view and atom numbering for (4). The displacement ellipsoids are drawn at 40% probability.

Table 4
Adenosine receptor affinities (Baraldi *et al.*, 2004) [K_i (nM)].

hA_1: displacement of specific [^{3}H]DPCPX binding at human A_1 receptors expressed in CHO cells; hA_{2A}: displacement of specific [^{3}H]ZM241385 binding at human A_{2A} receptors expressed in CHO cells; hA_{2B}: displacement of specific [^{3}H]DPCPX binding at human A_{2B} receptors expressed in HEK293 cells; hA_3: displacement of specific [^{3}H]MRE3008-F20 binding at human A_3 receptors expressed in CHO cells.

Compound	hA_1	hA_{2A}	hA_{2B}	hA_3	hA_1/hA_{2B}
(1)	200	>1000	5.5	>1000	36
(2)	>1000	>1000	24	>1000	–
(3)	900	>1000	35	>1000	26
(4)	448	>1000	39	>1000	11
(5)	>1000	>1000	>1000	>1000	–

1996). The flexible alignment method is a stochastic search procedure that simultaneously searches the conformation space of a collection of molecules and the space of alignments of those molecules; the scoring of alignments is based upon a Gaussian density representation of physico-chemical properties, such as aromaticity, the presence of hydrogen-bond donors and acceptors, partial charges *etc.* The best superposition result is shown in Fig. 7.

3. Results and discussion

The bond distances and angles of the xanthinic fragments, reported in Table 2, are quite similar and do not show significant discrepancies with the structural parameters of all other xanthines of known molecular structure. Compounds (3) and (5) are partially disordered: in (3) the C13—C14—C15 propyl group is disordered over two positions with occupancies of *ca* 0.5, as is the phenyl ring which is present inside the crystal in two almost equivalent positions nearly perpendicular to each other [the angle between the mean planes formed by the two rings: 87.5 (2)°]. In (5) the C12 terminal carbon of one propyl group and the C26 carbon of the phenyl group are disordered over two non-equivalent positions (refined occupancy factors: 0.73 and 0.61 for C12 and C26, respectively). The main intermolecular interactions involved in crystal formation are NH/OH···O/N and CH···O/N hydrogen bonding (Table 3) and van der Waals interactions. In general, we have considered the C—H···X (X = N,O) interactions where the H···X distance is less than 2.70 Å and C—H···X angle is greater than 130° to be significant.

The asymmetric unit of (1) is formed by a xanthinic molecule, a water molecule and a formylhydrazine molecule. Drug molecules display a planar conformation, stabilized by N—H···O, O—H···O and C—H···O contacts with the co-crystallized solvent molecules (see Table 3). They are linked in planes along the *b* direction by N7—H···O7 and O8—H···O4 hydrogen bonds; these planes being in turn linked by the water and the hydrazine molecules in a three-dimensional hydrogen-bond network.

Molecule (2) shows a packing where dimers are formed by N7—H···O2 hydrogen bonds. The dimers, in turn, are assembled in the crystalline lattice by dispersion forces. A similar packing pattern is shown by (3), which presents the same dimeric association as the previous structure. The dimers, in this case, are linked in chains running along the *c* direction by the N11—H···N10 hydrogen bond.

The packing architecture of (4) is quite complicated, in view of the relevant number of available hydrogen-bond donors and acceptors. The asymmetric unit contains two water and one dimethylformamide (DMF) molecules, in addition to the drug molecule. The carbonyl group of DMF forms a bifurcated hydrogen bond with N11—H and N12—H groups. The two water molecules are linked together and with their centrosymmetrically related molecules form a square, linking two drug molecules of different asymmetric units using the remaining H atoms.

Molecule (5) crystallizes with two water molecules, linked together, which in turn are connected to three molecules belonging to different asymmetric units, forming a complex three-dimensional packing pattern.

The five molecules, although chemically similar, exhibit different binding abilities to the four adenosinic receptors, as shown by the biological data reported in Table 4. Since generally the A_{2B} receptor subtype is in competition for the binding of the ligand mainly with the A_1 subtype, in the last

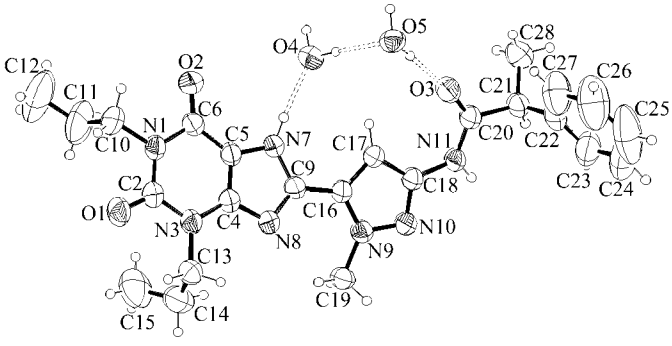

Figure 5
*ORTEP*III view and atom numbering for (5). The displacement ellipsoids are drawn at 40% probability. For the sake of clarity, only one component of the disordered groups is shown.

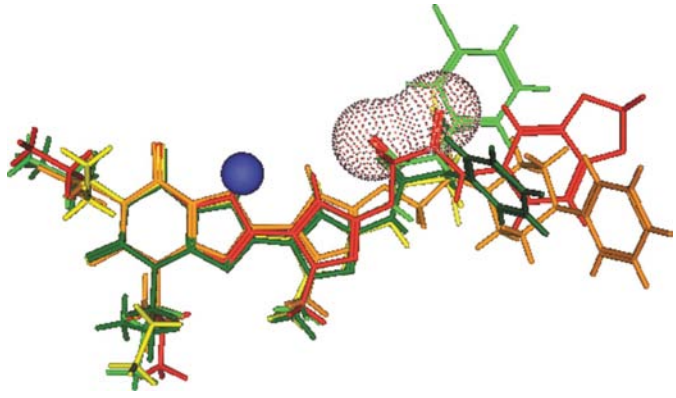

Figure 6
Superposition of the crystal structures of (1)–(5). (1): red; (2): orange; 3: yellow; (4): light green; (5): dark green. The blue sphere indicates the common N—H hydrogen-bond donor group, while Connolly dot surfaces indicate the carbonyl groups.

Table 5
Formula and adenosine-receptor affinities [K_i (nM)] for A_{2B} selective xanthinic antagonists (Kim *et al.*, 2000).

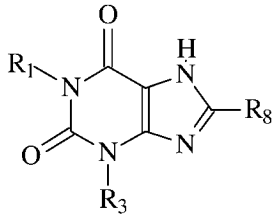

R_1	R_3	R_8	A_1	A_{2A}	A_{2B}	A_3	A_1/A_{2B}
$(CH_2)_2CH_3$	$(CH_2)_2CH_3$	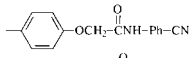	403	503	1.97	570	205
$(CH_2)_2CH_3$	$(CH_2)_2CH_3$	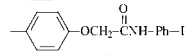	293	5140	2.13	1270	138
$(CH_2)_2CH_3$	$(CH_2)_2CH_3$	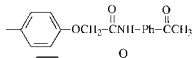	157	112	1.39	230	113
$(CH_2)_2CH_3$	$(CH_2)_2CH_3$	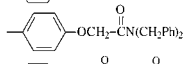	690	642	9.88	284	70
$(CH_2)_2CH_3$	$(CH_2)_2CH_3$	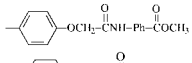	225	3100	3.93	363	57
$(CH_2)_2CH_3$	$(CH_2)_2CH_3$	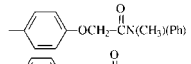	218	497	5.42	–	40
$(CH_2)_2CH_3$	$(CH_2)_2CH_3$	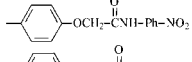	57	70	1.52	138	38
$(CH_2)_2CH_3$	$(CH_2)_2CH_3$	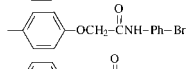	73.5	1640	2.35	2300	31
$(CH_2)_2CH_3$	$(CH_2)_2CH_3$	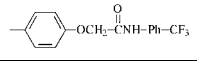	61.2	238	2.14	213	30

column of Table 4 the ratio between A_1 and A_{2B} affinity data is reported. The higher the value, the better the selectivity towards A_{2B}. In order to make the conformational differences of the five compounds in the crystalline state more evident we have superimposed their crystal structures in Fig. 6. Molecule (1) (highest affinity) is shown in red, while (5) (smallest affinity) is shown in dark green. The xanthinic moiety is almost identical in all the molecules, as confirmed by the data of Table 2; the N7—H hydrogen-bond donor group and the hydrogen-bond acceptor carbonyl group, shown respectively by a blue sphere and a Connolly dot surface, occupy almost the same position on the same side of the molecule. The main conformational differences are confined to the terminal part of the molecules, since they have, in principle, many rotational degrees of freedom around the single bonds of the chain. The conformation that a molecule adopts in the crystal depends mainly on its environment, *i.e.* the number and strength of the intermolecular interactions in the crystalline architecture.

The molecule showing the most peculiar behaviour is (5), which does not really bind to any of the four receptor subtypes, despite being identical, with the exception of the methyl substituent on the C21 atom, to (3), whose affinity to the A_{2B} receptor is conversely quite good (K_i = 35 nM). The different biological behaviour of the two molecules can be explained only in terms of steric encumbrance due to the methyl substituent that restricts the number of low-energy conformations accessible to the molecule. It can be hypothesized that this conformational limitation can be an obstacle to the correct entrance of the molecule into the active site, that might have a channel-like form, as shown by our recently reported docking simulation study (Ferretti & Bertoni, 2004).

The first two molecules, (1) in particular, seem to be very promising for a possible therapeutic use in view of their binding data. To explore in a more detailed way the structural features that most influence the molecule–macromolecule binding, we have searched the literature and have found nine xanthinic derivatives that display a very good binding affinity (Ka < 10 nM) and selectivity, similar to those of (1) whose formulae and biological data are reported in Table 5. Interestingly, a common feature of all the compounds is the presence of an aromatic ring at C9 (a phenyl ring instead of a pyrazole) substituted by an OCH_2CO*R* group, that on the contrary is missing in (3), (4) and (5). Since the crystallographic structures for these molecules are not available, their equilibrium geometries were obtained using the optimization procedure of the semiempirical quantum-mechanical program *MOPAC-PM3* (Stewart, 1989). A flexible alignment procedure was then utilized to superimpose all the molecules on (1), as described in §2 and shown in Fig. 7. Here the N—H hydrogen-bond donor group of the common xanthinic moiety is marked with a blue sphere, while dotted Connolly surfaces are used to represent the hydrogen-bond acceptor groups. The most evident structural similarity is the size of the molecules. Actually, the length of all of them in their extended conformation ranges from 21 to 25 Å. Moreover, although the substitutions are quite different in all the molecules, the alternation of hydrogen-bond donor and acceptor groups with

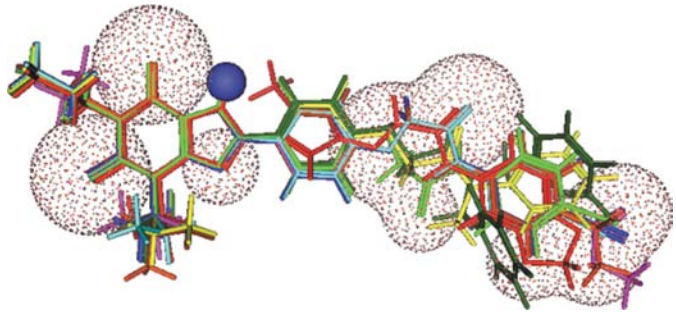

Figure 7
Molecules of Table 5 superimposed to (1). The blue sphere indicates the common N—H hydrogen-bond donor group, while Connolly dot surfaces indicate the hydrogen-bond acceptor groups.

lipophylic fragments is similar and in the final part of the molecules there is always an aromatic ring. These similarities can be seen in the light of a docking study we have recently published (Ferretti & Bertoni, 2004). In this study we have docked (1) to a model of the seven-helices bundle of the A_{2B} receptor obtained by Vriend (Vriend, 1990), localizing the possible binding pocket on the basis of the few site-mutagenesis studies presently available (Kim *et al.*, 1995; Olah *et al.*, 1992; Beukers *et al.*, 2000; Fredholm *et al.*, 2001). From these studies the Asn254 (TM6, *i.e.* belonging to the transmembranal chain 6), His251 (TM6) and His280 (TM7) residues appear to be conserved in all adenosine receptor subtypes and consequently they are believed to play an important role in the binding of both agonists and antagonists. A schematic view of the molecular–macromolecular interactions is shown in (I).

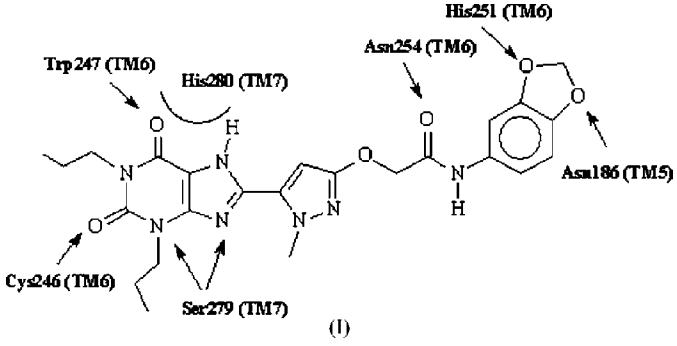

(I)

Interestingly, the spatial distance between the two histidines turns out to be 20 Å, *i.e.* the same length as the antagonists exhibiting high affinities to the A_{2B} receptor. The result of the docking procedure shows that the ligand binds to the protein through a number of specific interactions which can be classified as $X-H\cdots Y$ hydrogen bonds (X = S, N, O; Y = N,O), accounting for the good affinity data of (1). In particular, the xanthinic part of the molecule is located in the spatial region near the His280 (TM7) residue, while, on the opposite site, the antagonist is surrounded by the His251(TM6), Asn186 (TM5) and Asn254 (TM6) residues, the last one forming a hydrogen bond with the amidic carbonyl which is present in all the antagonists considered. In the simulation the benzoxyrane O atoms of (1) act as hydrogen-bond acceptors with respect to His251; the same role may be played, in principle, by the different substituents of the amidic nitrogen in all the molecules of Table 5 with the exception of the fourth and the sixth ones, which carry only aromatic groups in the same position. The superposition of such molecules to (1) when bound to the receptor has shown, nevertheless, that the phenyl rings could make hydrophobic interactions with many residues in the region of interest [for example, Phe134(TM4)], also stabilizing in this case the ligand–receptor binding. Moreover, a preliminary docking study on the same model of the receptor using the endogenous agonist adenosine as the ligand has shown that the number of specific adenosine–receptor interactions is few, since only the His251 and Asn254 residues appear to be involved in the binding. This fact leads to the conclusion that the large number of interactions the antagonists are able to form with the receptor account for their great affinity to it, when compared with the very low affinities of adenosine and other adenosinic agonists.

References

Altomare, A., Burla, M. C., Cavalli, M., Cascarano,G., Giacovazzo, C., Gagliardi, A., Moliterni, A. G., Polidori, G. & Spagna, R. (1999). *J. Appl. Cryst.* **32**, 115–121.

Baraldi, P. G., Cacciari, B., Borea, P. A., Varani, K., Pastorin, G., de Ros, T., Tabrizi, M. A., Fruttarolo, F. & Spallato, G. (2002). *Curr. Pharm. Des.* **6**, 2299–2332.

Baraldi, P. G., Tabrizi, M. A., Preti, D., Bovero, A., Romagnoli, R., Fruttarolo, F., Zaid, N. A., Moorman, A. R., Varani, K., Gessi, S., Meriggi, S. & Borea, P. A. (2004). *J. Med. Chem.* **6**, 1434–1447.

Beck-Sickinger, A. G. (1996). *DDT*, **1**, 502–513.

Beukers, M. W., den Dulk, H., van Tilburg, E. W., Brouwer, J. & Ijzerman, A. P. (2000). *Mol. Pharmacol.* **58**, 1349–1356.

Bruns, R. F., Lu, G. H. & Pugsley, T. A. (1986). *Mol. Pharmacol.* **29**, 331–346.

Burnett, M. N. & Johnson, C. K. (1996). *ORTEP*III. Report ORNL-6895. Oak Ridge National Laboratory, Oak Ridge, Tennessee, USA.

Chemical Computing Group Inc. (2003). *MOE (Molecular Operating Environment),* Release 2003.02. Chemical Computing Group Inc., Montreal, Canada.

Farrugia, L. J. (1999). *J. Appl. Cryst.* **32**, 837–838.

Ferretti, V. & Bertoni, E. (2004). *Minerva Biotecnol.* **16**, 79–84.

Fredholm, B. B., Ijzerman, A. P., Jacobson, K. J., Klotz, K.-N. & Linden, J. (2001). *Pharm. Rev.* **53**, 527–552.

Halgren, T. A. (1996). *J. Comput. Chem.* **17**, 616–641.

Halgren, T. A. & Nachbar, R. B. (1996). *J. Comput. Chem.* **17**, 587–615.

Hayallah, A. M., Sandoval-Ramirez, J., Reith, U., Schobert, U., Preiss, B., Schumacher, B., Daly, J. W. & Mueller, C. E. (2002). *J. Med. Chem.* **45**, 1500–1510.

Kim, J. H., Jiang, Q. L., Glashofer, M.., Yehle, S., Wess, J. & Jacobson, K. A. (1996). *Mol. Pharmacol.* **49**, 683–691.

Kim, J. H., Wess, J., van Rhee, A. M., Schoneberg, T. & Jacobson, K. A. (1995). *J. Biol. Chem.* **270**, 13987–13997.

Kim, S., Marshall, M. A., Melman, N., Kim, H. S., Mueller, C. E., Linden, J. & Jacobson, K. A.(2002). *J. Med. Chem.* **45**, 2131–2138.

Kim, Y.-C., de Zwart, M., Chang, L., Moro, S., von Frijtag Drabbe Kunzel, J., Melman, N., Ijzerman, A. P. & Jacobson, K. A. (1998). *J. Med. Chem.* **41**, 2835–2845.

Kim, Y.-C., Ji, X., Melman, N., Linden, J. & Jacobson, K. A. (2000). *J. Med. Chem.* **43**, 1165–1172.

Marquardt, D. L., Walker, L. L. & Heinemann, S. (1994). *J. Immunol.* **152**, 4508–4515.

Miller, M. D., Sheridan, R. P. & Kearsley, S. K. (1999). *J. Med. Chem.* **42**, 1505–1514.

Nardelli, M. (1995). *J. Appl. Cryst.* **28**, 659.

Nonius (1997). *Kappa-CCD Server Software.* Nonius BV, Delft, The Netherlands.

Olah, M. E., Ren, H. Z., Ostrowski, J., Jacobson, K. A. & Stiles, G. L. (1992). *J. Biol. Chem.* **267**, 10764–10770.

Otwinowski, Z. & Minor, W. (1997). *Methods Enzymol.* **276**, 307–326.

Palczewski, K., Kumasaka, T., Hori, T., Behnke, C. A., Motoshima, H., Fox, B. A., Le Trong, I., Teller, D. C., Okada, T., Stenkamp, R. E., Yamamoto, M. & Miyano, M. (2000). *Science*, **289**, 739–745.

Pierce, K. D., Furlong, T. J., Selbie, L. A. & Shine, J. (1992). *Biochem. Biophys. Res. Commun.* **187**, 86–93.

Ralevic, V. & Burnstock, G. (1998). *Pharm. Rev.* **50**, 413–477.

Rivkees, S. A. & Reppert, S. M. (1992). *Mol. Endocrinol.* **6**, 1598–1604.

Sheldrick, G. M. (1997). *SHELX*97. University of Göttingen, Germany.
Stewart, J. J. P. (1989). *J. Comput. Chem.* **10**, 209–220.
Vriend, G. (1990). *J. Mol. Graph.* **8**, 52–56.
Wildman, S. A. & Crippen, G. M. (1999). *J. Chem. Inf. Comput. Sci.* **39**, 868–873.